AD-A286 507

.TION PAGE Dist: A

1. AGENCY USE ONLY (Leave blank)	2. REPORT DATE August 1994	3. REPORT TYPE AND DATES COVERED Reprint

4. TITLE AND SUBTITLE

Shock wave interactions in hypervelocity flow (u)

5. FUNDING NUMBERS

PE - 61103D
PR - 3484
SA - AS
G - F49620-93-1-0338

6. AUTHOR(S)

S. R. Sanderson and B. Sturtevant

7. PERFORMING ORGANIZATION NAME(S) AND ADDRESS(ES)

California Institute of Technology
1201 E. California Blvd.
Pasadena, CA 91125

8. PERFORMING ORGANIZATION REPORT NUMBER

AFOSR-TR- 94 0727

9. SPONSORING/MONITORING AGENCY NAME(S) AND ADDRESS(ES)

AFOSR/NA
110 Duncan Avenue, Suite B115
Bolling AFB DC 20332-0001

10. SPONSORING/MONITORING AGENCY REPORT NUMBER

11. SUPPLEMENTARY NOTES

Proceedings of the 19th International Symposium on Shock Waves, Marseille, France July, 1994.

12a. DISTRIBUTION/AVAILABILITY STATEMENT

Approved for public release; distribution is unlimited

12b. DISTRIBUTION CODE

A

13. ABSTRACT (Maximum 200 words)

Abstract. The impingement of shock waves on blunt bodies in steady supersonic flow is known to cause extremely high local heat transfer rates and surface pressures. Although these problems have been studied in cold hypersonic flow, the effects of dissociative relaxation processes are unknown. In this paper we report a model aimed at determining the boundaries of the possible interaction regimes for an ideal dissociating gas. Local analysis about shock wave intersection points in the pressure-flow deflection angle plane with continuation of singular solutions is the fundamental tool employed. Further, we discuss an experimental investigation of the nominally two-dimensional mean flow that results from the impingement of an oblique shock wave on the leading edge of a cylinder. The effects of variations in shock impingement geometry were visualized using differential interferometry. Generally, real gas effects are seen to increase the range of shock impingement points for which enhanced heating occurs. They also reduce the type IV (Edney 1968 a,b) interaction supersonic jet width and influence the type II-III transition process.

DTIC QUALITY INSPECTED 3

14. SUBJECT TERMS

shock-on-shock interaction, shock impingement, hypervelocity flow, dissociation, relaxation, heat transfer

15. NUMBER OF PAGES 12

16. PRICE CODE

17. SECURITY CLASSIFICATION OF REPORT	18. SECURITY CLASSIFICATION OF THIS PAGE	19. SECURITY CLASSIFICATION OF ABSTRACT	20. LIMITATION OF ABSTRACT
Unclassified	Unclassified	Unclassified	UL

Best
Available
Copy

Shock wave interactions in hypervelocity flow

S. R. Sanderson and B. Sturtevant

California Institute of Technology, Pasadena, CA 91125, USA

Abstract. The impingement of shock waves on blunt bodies in steady supersonic flow is known to cause extremely high local heat transfer rates and surface pressures. Although these problems have been studied in cold hypersonic flow, the effects of dissociative relaxation processes are unknown. In this paper we report a model aimed at determining the boundaries of the possible interaction regimes for an ideal dissociating gas. Local analysis about shock wave intersection points in the pressure–flow deflection angle plane with continuation of singular solutions is the fundamental tool employed. Further, we discuss an experimental investigation of the nominally two-dimensional mean flow that results from the impingement of an oblique shock wave on the leading edge of a cylinder. The effects of variations in shock impingement geometry were visualized using differential interferometry. Generally, real gas effects are seen to increase the range of shock impingement points for which enhanced heating occurs. They also reduce the type IV (Edney 1968 a,b) interaction supersonic jet width and influence the type II–III transition process.

1. Introduction

Shock impingement phenomena, which inhibit the further development of hypervelocity vehicles, are discussed in the literature by many authors, notably by Edney (1968 a,b). For the inviscid, compressible flow of a perfect gas a sufficient set $\acute{o}$ of dimensionless parameters to describe any quantity in the flow is, $\varphi = \phi[M, \gamma, \beta_1, \Lambda, \Gamma]$, where M is the free stream Mach number, γ is the ratio of specific heats, β_1 is the impinging shock wave angle, Λ describes the position of the impinging shock wave with respect to the body and Γ is a set of parameters defining the body geometry. Consider the case of a given gas and fixed free stream condition, impinging shock strength and body geometry. The only remaining dependence is then the location of the impingement point relative to the body, i.e., $\phi = \phi[\Lambda]$. As the incident shock wave is translated relative to the body it potentially intersects with all possible shock strengths of both positive and negative slope. On the basis of an experiment such as this, with spherical and modified spherical bodies, Edney (1968 a,b) observed and categorized six interaction regimes; known as types I–VI. Edney rationalized the observed flow fields through local analysis about shock wave intersection points in the pressure–flow deflection angle plane (p-δ plane). The key conclusion drawn from such an analysis is the role of the three-shock solutions (or λ-shocks) and this is discussed further in §2. Based on the assumption of straight shocks in the vicinity of the interaction, conclusions were drawn about the global nature of the flow. When the impinging shock wave is weak, the flow downstream of a λ-shock is characterised by low Mach number flow behind the strong transmitted wave and high Mach number flow downstream of the weak reflected shock. On dimensional grounds, the inertia of the supersonic stream is dominant. Thus, the flow field for the global type IV interaction, whereby a supersonic jet penetrates a region of low subsonic flow [see Edney (1968 a,b) or Fig. 4], can be solved approximately as a free streamline flow up to some unknown length scale. Typically this length scale is specified in terms of the width of the jet.

According to Edney's model, the heat transfer is determined by the attachment at the body surface of the shear layers generated at the shock impingement points. A correlation was obtained between local pressure and local heat transfer rate at the surface. A further observation made by Edney is that the jet curvature increases as the intersection point moves up. Some recent contributions to the literature are noted in the references of this paper.

2. Local analysis for an ideal dissociating gas

The flow in smooth regions and across shock discontinuities is, in principle, understood. The predominant concern is then points where surfaces of discontinuity intersect. Local analysis about intersection points in the p-δ plane provides a useful tool for analysis. This technique is well known in the Mach reflection literature—see for example Hornung (1986). Our purpose here is to generalize these tools to the case of oblique translational shock waves where both the upstream and

1

downstream conditions are non-equilibrium states with respect to the internal degrees of freedom of the gas. This analysis is performed for a one-dimensional shock and subsequently extended to oblique waves.

Consider the dimensionless form of the continuity and momentum equations that apply across a one-dimensional translational discontinuity and throughout the downstream relaxation zone,

$$\hat{\rho}\hat{u} = 1 \, , \qquad \hat{p} = 1 + \frac{1}{P}\frac{\hat{\rho}-1}{\hat{\rho}} \, , \tag{1,2}$$

where $P = p_1/\rho_1 u_1^2$. The symbols have the usual meanings and generally $\hat{\phi} = \phi_2/\phi_1$.

We use Lighthill's (1957) model for the thermodynamics of an ideal dissociating gas (IDG):

$$p = \frac{k}{2m}(1+\alpha)\rho T \, , \qquad h = \frac{k}{2m}[(4+\alpha)T + \alpha\theta_d] \, , \tag{3,4}$$

where k is Boltzmann's constant, m is the mass of one atom of the gas, θ_d is a temperature characterizing the dissociation energy and α is the dissociated mass fraction. Using equation (4) the dimensionless energy conservation equation becomes,

$$(4+\alpha_2)\frac{T}{D} + \alpha_2 + \frac{K}{\hat{\rho}^2} = H_0 \, , \tag{5}$$

where the dimensionless parameters are $D = \theta_d/T_1$, $K = mu_1^2/k\theta_d$ and $H_0 = 2mh_0/k\theta_d$. H_0 is the conserved stagnation enthalpy.

Importantly, for a nonequilibrium binary mixture, three parameters are sufficient to define the thermodynamic state of the upstream gas. Here we specify P, H_0 and α_1. The remaining parameters are then given by the following identities, obtained from H_0 written in terms of conditions upstream of the discontinuity,

$$K = \frac{H_0 - \alpha_1}{1 + 2P\frac{4+\alpha_1}{1+\alpha_1}} \qquad D = \frac{4+\alpha_1}{H_0 - K - \alpha_1} \, . \tag{6,7}$$

From equation (3) it follows that $T = \frac{\hat{p}(1+\alpha_1)}{\hat{\rho}(1+\alpha_2)}$ and, eliminating T and D from equation (5), with the pressure given by (2), leads to the following quadratic equation for the density,

$$(H_0 - \alpha_2)\hat{\rho}^2 - \frac{\lambda(P+1)}{P}\hat{\rho} + \frac{\lambda - KP}{P} = 0 \, , \qquad \lambda = 2KP\frac{4+\alpha_2}{1+\alpha_2} \, . \tag{8}$$

One solution describes the variation of density downstream of a translational shock. The remaining solution describes relaxation of the (possibly) nonequilibrium upstream state without any discontinuity. Both solutions are parameterized in terms of the dissociation mass fraction α_2, whose rate of reaction need not yet be specified. This interpretation for the case $\alpha_1 = 0$ is due to Hornung (1979).

Equation (8) may be combined with an equilibrium expression to obtain the asymptotic state far downstream from the translational shock. For the equilibrium IDG,

$$\frac{\alpha_{2_{eq}}^2}{1 - \alpha_{2_{eq}}} = \frac{\hat{\rho}_d}{\hat{\rho}}e^{-D/\hat{T}} \, . \tag{9}$$

This leads to a second transcendental equation relating α_2 and ρ. Numerically solving equation (8) with $\alpha_2 = \alpha_{2_{eq}}$ given by (9) gives the equilibrium shock solution for specified upstream conditions P, H_0 and α_1. Further, solving equation (8) with $\alpha_2 = \alpha_1$ gives the frozen solution valid immediately downstream of the translational discontinuity.

The extension to oblique shock waves is obtained in the usual way. The normal components, of P and K are given in terms of β the angle of the oblique shock wave by

$$P_{1_N} = \frac{P_1}{\sin^2\beta} \, , \qquad K_{1_N} = K_1\sin^2\beta \, . \tag{10,11}$$

2

These are used in (6), (8), (9) and (2), and the the flow deflection angle δ is determined from $\hat{\rho} = \tan\beta/\tan(\beta - \delta)$.

To facilitate the computation of multiple shock jumps for the interaction problem we must find a convenient means of determining P and H_0 downstream of the oblique shock. Trivially $H_{0_2} = H_{0_1}$. It can be sh⋯ that $K_2 = K_1(\cos^2\beta + \sin^2\beta/\hat{\rho}^2)$. P_2 then follows from (6).

3. Continuation of s⋯ r solutions

While the p-δ plane r⋯ ⋯ntation is useful for interpretation of solutions it is difficult to deal with the case distinctions that arise as the number of parameters is increased. One technique for reducing the amount of information is to consider only the singular cases that delineate regions of solutions with similar forms. Various special cases arise that are significant in terms of transition to Mach reflection. Discussion of the significance of these points can be found in the literature [e.g., Hornung (1986)]. Now generalize these cases to the asymmetrical interaction of oblique shock waves;

i. Interaction of shock waves that produce a Mach stem with zero curvature. This is a generalization of the von Neumann condition in Mach reflection.

ii. Sonic flow downstream of the transmitted shock waves.

iii. Coalescence of the strong and weak regular solutions such that the shock loci intersect only tangentially. This is a generalization of the maximum deflection condition in Mach reflection.

iv. Sonic flow downstream of the incident shock waves.

v. One transmitted shock wave—λ-shocks.

Given the solution for one such set of these singular points, solutions for neighboring values of the parameters may be determined using path following techniques [see Keller (1987)] for either frozen or equilibrium chemistry. The frozen solution applies in regions near the shock wave intersection point and the equilibrium solution is valid far from the shock waves. The regular 4-shock intersections map into the 2nd and 4th quadrants of Fig. 1 and lie on the surface bounded by the axes and the von Neumann curves. Outside this region the only solutions are the λ-shocks which exist only along lines. If the impingement point on a blunt body maps to a region of Fig. 1 where no regular solution exists then the flow must deform in such a way that the λ-shock condition is maintained at the intersection point. This highlights the physical mechanism determining the gross nature of the flow field.

It is interesting to consider various classical problems in this framework. a) Shock detachment from a wedge; $\sigma_1 = \sigma_2$. Hornung and Smith (1979) observed significant non-equilibrium effects. This is consistent with the separation of the frozen and equilibrium sonic lines in Fig. 1. b) Mach reflection; $\sigma_1 = -\sigma_2$. Hornung et al. (1979) observed that non-equilibrium effects were slight. This is consistent with the proximity of the frozen and equilibrium von Neumann lines in Fig. 1. c) Shock impingement problem; $\sigma_1 = const$. Little experimental evidence exists for high enthalpy effects in this case. For weak impinging shock waves, shown by the vertical line in Fig. 1, the separation of the frozen and equilibrium λ-shock solutions is relatively large. This suggests some effect on the transition from type II to type III. This occurs in the vicinity of the sonic line which is itself sensitive to non-equilibrium processes.

4. Experimental results

We have conducted an experimental investigation of the nominally two-dimensional mean flow that results from the impingement of an oblique shock wave on the leading edge of a cylinder. This problem is abstracted from the complex configurations which occur in the flow about flight vehicles and contains much of the physics. These initial experiments, comprising 35 shots, were conducted in the GALCIT T5 free piston reflected shock tunnel with nitrogen test gas at nozzle reservoir enthalpies of 3 MJ/kg and 12.5 MJ/kg and reservoir pressures of 12 MPa and 25 MPa, respectively. The reservoir gas was expanded through a contoured axisymmetric nozzle with area ratio 109.5 to yield a nominal Mach number of 5.5 in the test section. The cylinder was 37.5 mm in diameter with aspect ratio 4.5 and the flow was deflected 7 degrees by the incident planar shock wave. The effects of variations in shock impingement geometry were visualized using infinite fringe differential interferometry with vertical beam shear. A Q-switched, frequency doubled, NdYAG laser was used as the light source.
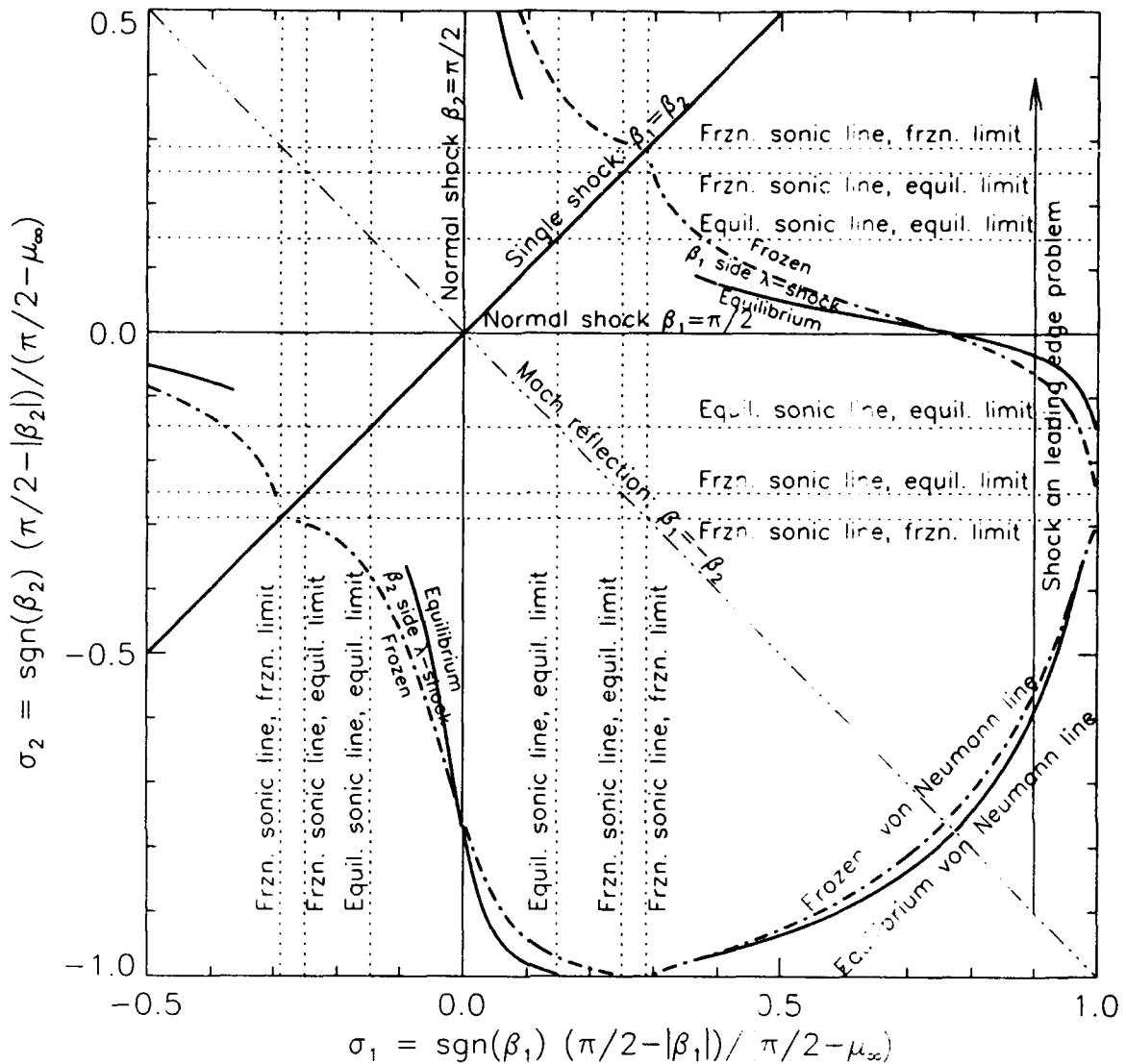
3

Fig. 1. Map of interaction regimes for two intersecting oblique shock waves of angles β_1 and β_2. Shock angles are normalized so that $\sigma = 0$ corresponds to a normal shock wave. Mach waves correspond to $\sigma = \pm 1$. The free stream conditions are taken as $H_0 = 0.5$, $P = 0.03$ (or $M_\infty = 5$ with $\gamma = 4/3$), $\alpha_1 = 0$ and $\hat{\rho}_d = 10^6$.

Figs. 2–4 illustrate type II, III and IV interactions at stagnation enthalpies of 3 MJ/kg and 12.5 MJ/kg. The incident shock is concave down at the edge of test section and some fringe shift is observed below this wave. This complicates interpretation of the images. However, the main centerline disturbance is generally at the top of the line-of-sight-integrated image.

At the lowest impingement point reported in this paper the type I–II transition has already occurred with the incident shock wave impinging somewhat below the lower sonic line (Fig. 2). In the low enthalpy case a Mach stem connects the λ-shock pattern at the impingement point to the bow shock of the cylinder. At the intersection point a strong vortex sheet is generated separating the upper region of subsonic flow from the lower region of supersonic flow. No transmitted wave is resolvable at the upper end of the Mach stem which appears to join smoothly into the bow shock in the vicinity of the sonic line. The upper portion of the bow shock remains symmetrical. In the high enthalpy case the bow shock remains undisturbed. However, a point of inflection is observed immediately above the intersection point.
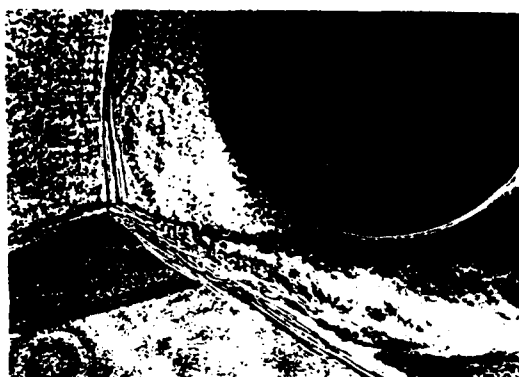
4

(a) 3 MJ/kg   (b) 12.5 MJ/kg

Fig. 2 Differential interferograms of type II interactions.

(a) 3 MJ/kg   (b) 12.5 MJ/kg

Fig. 3 Differential interferograms of type III interactions.

In the type III experiments (Fig. 3) the incident shock wave intersects the bow shock wave in the subsonic region, somewhat below the geometric stagnation point. For both enthalpies the Mach stem has merged with the bow shock wave and the λ-shock pattern is preserved at the intersection point. The influence of the impinging shock wave is now global and both the radius of curvature and the standoff distance of the asymmetrical upper portion of the bow shock has increased to match the λ-shock pattern at the impingement point. Dominated by the inertia of the supersonic stream, the shear layer is deflected only in the immediate vicinity of the cylinder (c.f. discussion in §1). Generally, the standoff distance decreases with increasing enthalpy and this influences the impingement of the shear layer on the body. In the high enthalpy case, the resulting compression waves, that are observed as a series of nearly vertical white lines below the impingement point, steepen the lower shock. Kinks are observed where these waves meet the supersonic continuation of the bow shock. Weak reflected expansions are observed as horizontal disturbances emanating from the intersection points. Note the analogy between this phenomenon and the mechanism of complex Mach reflection.

When the incident shock wave impinges in the vicinity of the geometrical stagnation point a type IV flow results (Fig. 4). The λ-shock pattern is preserved and the supersonic transmitted portion of the bow shock forms a second inverted λ-shock with the subsonic continuation of the bow shock below the interaction. The flow behind the oblique shock wave connecting the two λ-shocks is supersonic and forms a jet that turns upwards under the action of the pressure gradient produced by the second λ-shock. The strongly curved shear layer generated at the upper λ-shock forms large plumes as it passes above the cylinder. The standoff distance and jet width are reduced in the high enthalpy case but this also depends strongly on the location of the impinging shock. A portion of the supersonic flow is now turned so that it passes above the cylinder and hence the stagnation streamline must pass through the supersonic jet. The stagnation density is higher for streamlines that pass through the supersonic jet than for streamlines that cross the adjacent strong

5

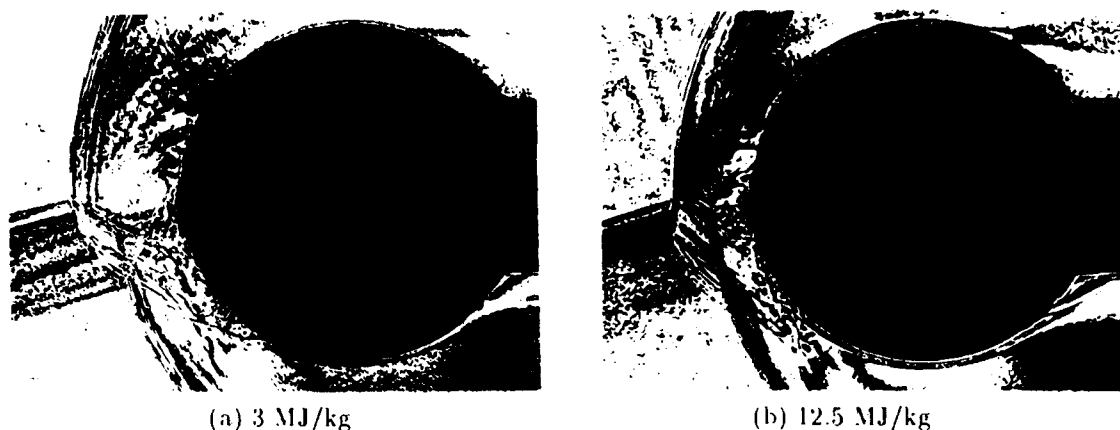(a) 3 MJ/kg   (b) 12.5 MJ/kg

Fig. 4 Differential interferograms of type IV interactions.

bow shock. The higher density and large unsteady velocity gradients produced by the impingement of the supersonic jet provide the mechanism for local increase of the heat transfer rate.

5. Conclusions

Local analysis about shock wave intersection points in the p-δ plane has been extended to the ideal dissociating gas model. The application of continuation methods to singular solutions illustrated the role of λ-shocks and determined the influence of real gas effects on local analysis. Experiments conducted in a free piston shock tunnel provided insight into real gas effects on the global flow. Generally, real gas effects are seen to increase the range of shock impingement points for which enhanced heating occurs. They further influence the Mach stem form in type II flows, the deflection of the shear layer in type III flows and the length scales associated with the type IV jet.

Acknowledgement

References

Delery JM (1990) Shock Interference Phenomena in Hypersonic Flows. Third Joint Europe/US Short Course in Hypersonics, RWTH Aachen.

Edney BE (1968a) Effects of Shock Impingement on the Heat Transfer Around Blunt Bodies. AIAA Jour 6:15–21.

Edney BE (1968b) Anomalous heat transfer and pressure distributions on blunt bodies at hypersonic speeds in the presence of an impinging shock. FFA-115, The Aeronautical Research Institute of Sweden.

Hornung HG (1972) Non-equilibrium dissociating nitrogen flow over spheres and circular cylinders. J Fluid Mech 53:149–176.

Hornung HG (1986) Regular and Mach reflection of shock waves. Ann Rev Fluid Mech 18:33–58.

Hornung HG, Oertel H and Sandeman RJ (1979) Transition to Mach reflexion of shock waves in steady and pseudosteady flow with and without relaxation. J Fluid Mech 90:541.

Hornung HG and Smith GH (1979) The influence of relaxation on shock detachment. J Fluid Mech 93:225.

Keller HB (1987) Numerical methods in bifurcation problems. Springer-Verlag.

Klopfer GH and Yee HC (1988) Hypersonic shock-on-shock interaction on blunt cowl lips. AIAA Paper 88-0233.

Lighthill MJ (1957) Dynamics of a dissociating gas. Part I. Equilibrium flow. J Fluid Mech 2:1–32.

Wieting AR and Holden MS (1989) Experimental shock wave interference heating on a cylinder at Mach 6 and 8. AIAA Jour 27:1557–1565.
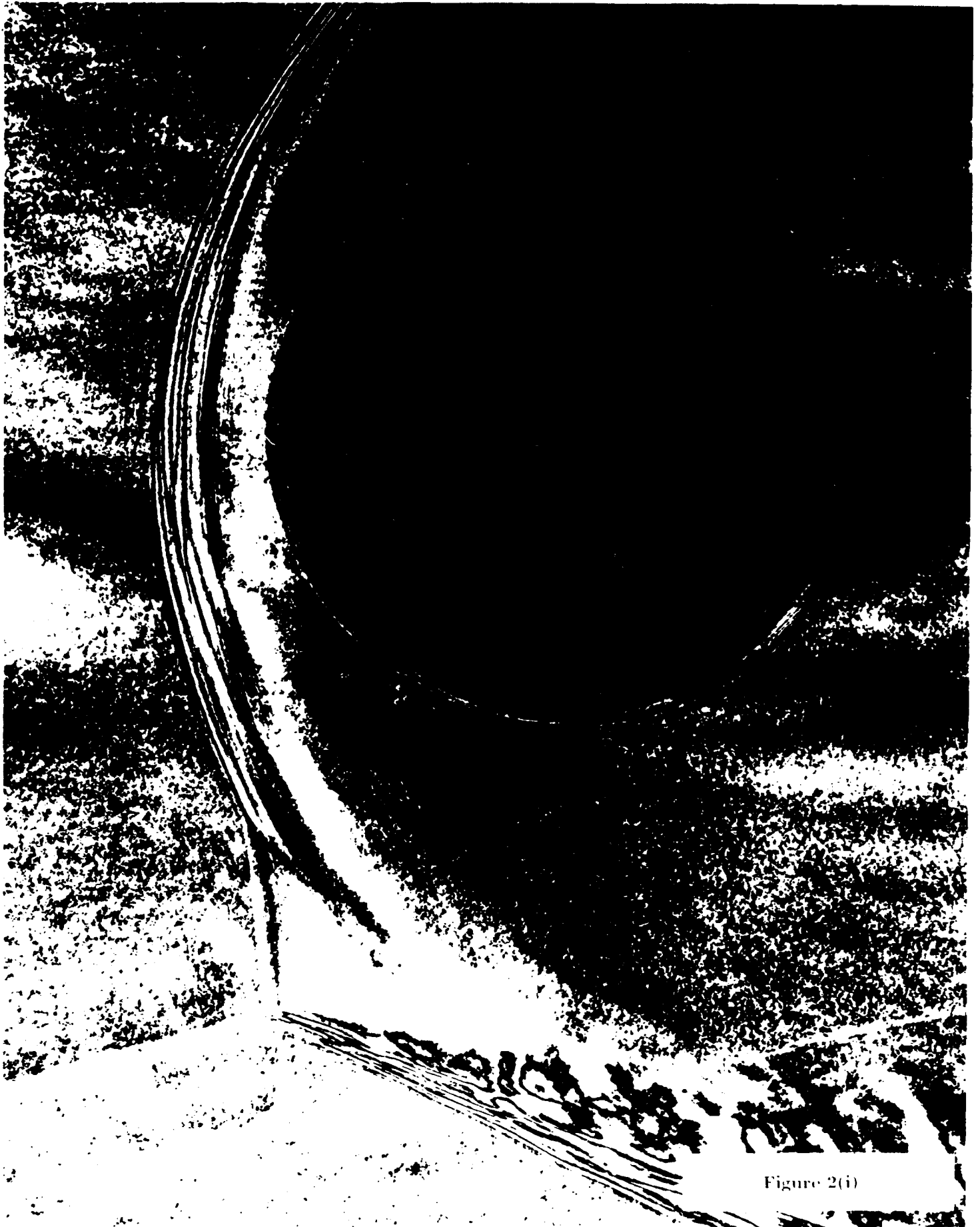
Figure 2(i)

Figure 2(ii)

Figure 3(i)

Figure 3(ii)

Figure 4(i)

Figure 4(ii)